Pediatr Radiol (2017) 47:1707–1720
DOI 10.1007/s00247-017-3927-5

REVIEW

Role of magnetic resonance urography in pediatric renal fusion anomalies

Sherwin S. Chan[1] · **Aikaterini Ntoulia**[2] · **Dmitry Khrichenko**[2] · **Susan J. Back**[2,3] · **Gregory E. Tasian**[3,4] · **Jonathan R. Dillman**[5] · **Kassa Darge**[2,3]

Received: 27 February 2017 / Revised: 10 May 2017 / Accepted: 9 June 2017 / Published online: 24 August 2017

Abstract Renal fusion is on a spectrum of congenital abnormalities that occur due to disruption of the migration process of the embryonic kidneys from the pelvis to the retroperitoneal renal fossae. Clinically, renal fusion anomalies are often found incidentally and associated with increased risk for complications, such as urinary tract obstruction, infection and urolithiasis. These anomalies are most commonly imaged using ultrasound for anatomical definition and less frequently using renal scintigraphy to quantify differential renal function and assess urinary tract drainage. Functional magnetic resonance urography (fMRU) is an advanced imaging technique that combines the excellent soft-tissue contrast of conventional magnetic resonance (MR) images with the quantitative assessment based on contrast medium uptake and excretion kinetics to provide information on renal function and drainage. fMRU has been shown to be clinically useful in evaluating a number of urological conditions. A highly sensitive and radiation-free imaging modality, fMRU can provide detailed morphological and functional information that can facilitate conservative and/or surgical management of children with renal fusion anomalies. This paper reviews the embryological basis of the different types of renal fusion anomalies, their imaging appearances at fMRU, complications associated with fusion anomalies, and the important role of fMRU in diagnosing and managing children with these anomalies.

Keywords Children · Functional magnetic resonance urography · Kidney · Magnetic resonance imaging · Renal fusion abnormalities · Urinary tract

Introduction

Renal ectopy and fusion are on a spectrum of congenital abnormalities that occur due to disruption of the migration process of the embryonic kidneys from the pelvis to the retroperitoneal renal fossae [1, 2]. Renal ectopia can be simple, crossed with or without renal fusion, or fused in the midline. Simple renal ectopia occurs when the kidney is not located in its expected position in the retroperitoneal renal fossa, and usually refers to a low-lying pelvic kidney that failed to ascend normally. In crossed renal ectopia, one kidney crosses over the midline and lies in the opposite side of the abdomen relative to its ureteral insertion. Most kidneys that cross the midline fuse with the contralateral kidney, a condition referred to as crossed-fused ectopia. Horseshoe kidney is a specific type of renal fusion anomaly in which the lower poles of the kidneys are joined in the midline, but each distinct renal unit remains on either side of the midline [1, 3–5]. This review will focus on renal fusion anomalies. Renal fusion anomalies are clinically important because they are associated with increased risk for complications, such as urinary tract obstruction, infection and urolithiasis [1, 2, 6]. Patients are also at increased risk for renal injuries during blunt abdominal trauma because the kidneys are located away from their normal location under the ribs and can be compressed against the spine [7, 8].

✉ Sherwin S. Chan
sschan@cmh.edu

[1] Department of Radiology, Children's Mercy Hospital, 2401 Gillham Road, Kansas City, MO 64108, USA

[2] Division of Body Imaging, Department of Radiology, The Children's Hospital of Philadelphia, Philadelphia, PA, USA

[3] Perelman School of Medicine, University of Pennsylvania, Philadelphia, PA, USA

[4] Division of Urology, Department of Surgery, The Children's Hospital of Philadelphia, Philadelphia, PA, USA

[5] Division of Thoracoabdominal Imaging, Department of Radiology, Cincinnati Children's Hospital Medical Center, Cincinnati, OH, USA

These anomalies are most commonly imaged using ultrasound (US) for anatomical definition and some are then imaged using renal scintigraphy to quantify renal function and assess urinary tract drainage. Functional magnetic resonance urography (fMRU) is an advanced imaging technique that combines the excellent soft-tissue contrast of conventional MRI with quantitative assessment based on contrast medium uptake and excretion kinetics to provide information on renal function and drainage. fMRU has been shown to be clinically useful in evaluating a number of urological conditions [9–11].

Renal fusion anomalies have been described on nuclear medicine studies, US, intravenous urography and computed tomography (CT) but have not been described in detail using fMRU [1, 2]. This paper reviews the embryology of renal fusion anomalies, their appearance on fMRU, complications associated with fusion anomalies, and the role of fMRU in their diagnosis and management in children.

Embryology

Understanding normal renal development aids the interpretation of anatomical variations and structural malformations of the kidneys [12–15]. The embryonic kidney goes through three distinct phases: pronephros, mesonephros and metanephros. The permanent kidney develops from the metanephros. It arises caudal to the mesonephros and has a dual composition: the epithelial cells of the ureteric bud and the mesenchymal cells of the metanephric blastema [16]. The ureteric bud arises as a branch of the distal part of the mesonephric duct. The bud then elongates and its tip penetrates the metanephric blastema (Fig. 1). A series of signaling interactions between these tissues causes the ureteric bud to branch multiple times to form the ureter, renal pelvis, calyces and collecting tubules (Fig. 1). At the same time, the metanephric blastema undergoes epithelial conversion, induced by the adjacent ureteric bud branch tips, to form nephrons that are comprised of a glomerulus, proximal and distal convoluted tubules, and a loop of Henle.

Between the sixth and eighth embryonic week, the permanent kidneys migrate cephalad from their site of origin in the presacral region into the renal fossae in the paralumbar region. The ascent of the kidneys occurs due to true migration as well as growth of the lumbar portion of the fetal body. The kidneys reach their final level by the end of the eighth week of gestation. During their ascent from the pelvis, the kidneys rotate medially approximately 90^0 around their longitudinal axis before they assume their final position. Over the course of ascension, the renal blood supply is sequentially supplied from neighboring vessels. Initially, blood flow is from the middle sacral artery, followed by the common iliac and inferior mesenteric arteries, and finally the abdominal aorta. Venous drainage from the kidneys is often also anomalous.

Types of renal fusion anomalies

Failure of ascension results in renal ectopia [17]. In simple renal ectopia, the affected kidney is in an abnormal position but on the proper side of the body and can be in the pelvis, at the level of the iliac wing or rarely in the thorax. Crossed renal ectopia occurs when the affected kidney crosses the midline and lies on the opposite side of the body. The ureter associated with the crossed kidney, however, inserts at its normal position on the bladder. When the crossed kidney fuses with the contralateral one it is called crossed-fused renal ectopia. If renal fusion occurs along the lower pole of the kidneys but the kidneys remain on their respective sides of the midline, the result is a horseshoe kidney. Renal fusion ectopias are commonly associated with other urinary tract and congenital abnormalities.

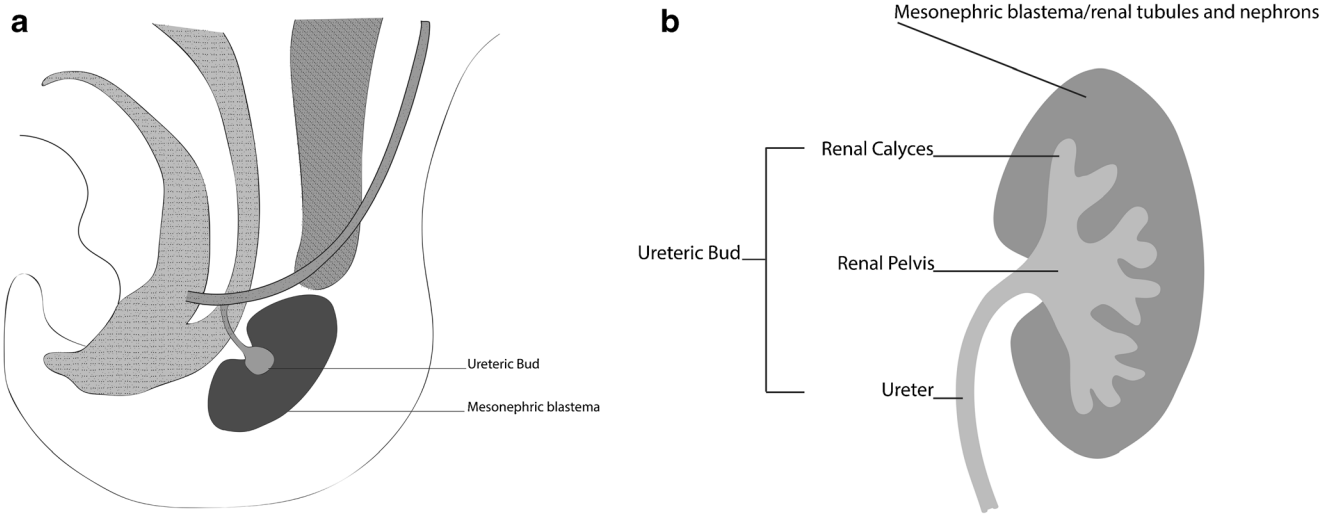

Fig. 1 Illustration of renal development. **a** Embryological diagram shows the ureteric bud invaginating into the mesonephric blastema. **b** The bud differentiates into the renal collecting system and the blastema differentiates into the nephrons and tubules after ascending. Renal fusion anomalies occur when the right and left blastema fuse together during their ascent. Images created by Jessica F. Yim

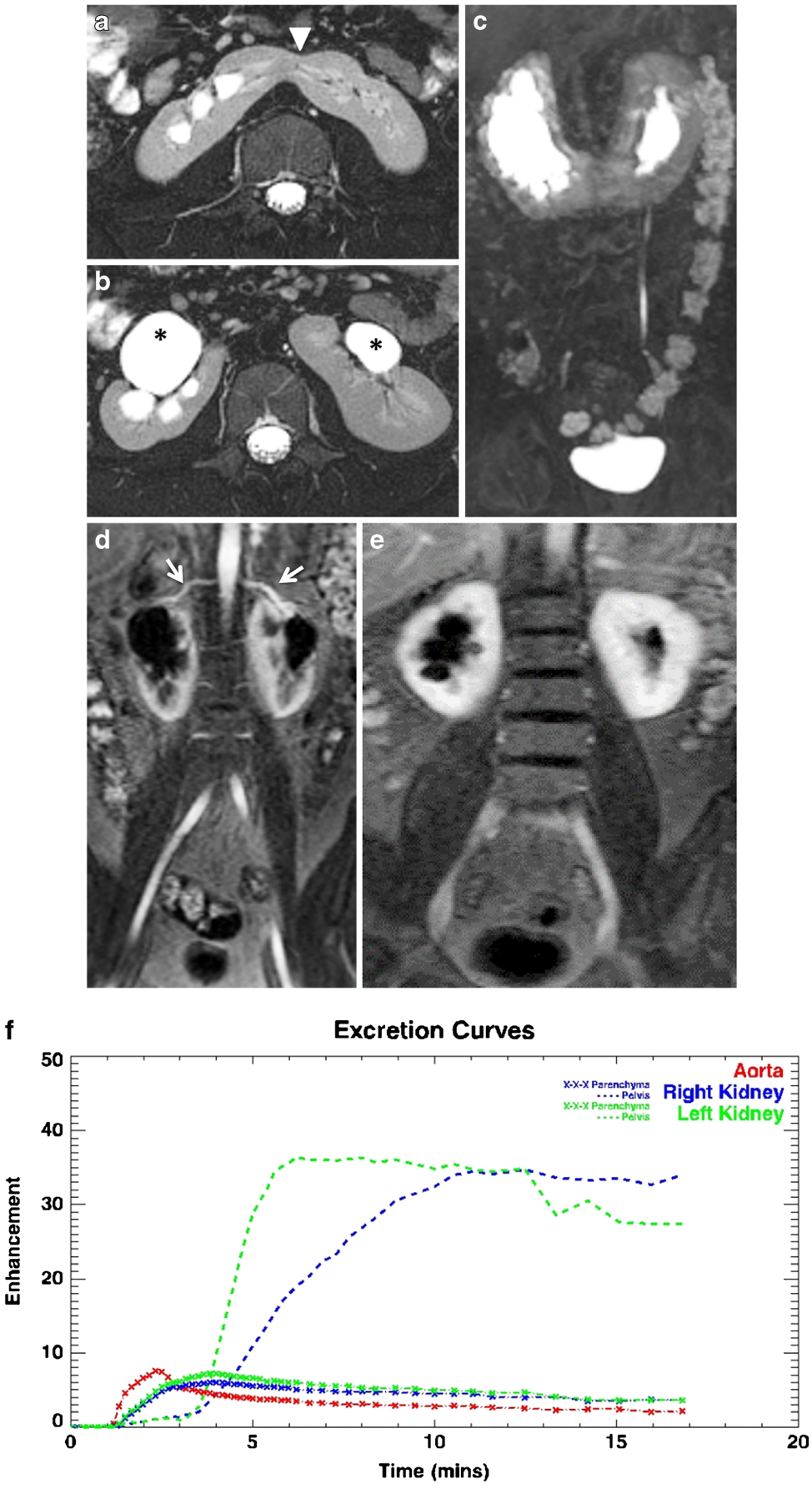

Fig. 2 An 8-year-old male with a horseshoe kidney and bilateral renal collecting system dilation. **a** Axial T2-weighted fat-suppressed image shows fusion of the inferior poles of the right and left renal moieties in the midline *(arrowhead)* with a bridging isthmus of normal renal tissue. The renal parenchyma has normal signal intensity and normal corticomedullary differentiation. **b** Each kidney has an extrarenal pelvis morphology *(asterisks)* that points anteriorly and has dilation of the left pelvis and dilation of the right pelvis and central calyces. **c** Coronal maximum intensity projection from a volumetric T2-weighted fat-saturated acquisition redemonstrates renal collecting system dilation and shows right cortical thinning with no dilation of the ureters. **d** Arterial phase post-contrast coronal T1-weighted fat-suppressed image shows prompt enhancement of a single artery on each side (*arrows*), which courses above the level of the renal pelvises. **e** Delayed post-contrast coronal T1-weighted fat-suppressed image shows that contrast washout is symmetrical with no overt obstruction identified. **f** Note the symmetry in the enhancement curves. The cortical transit times were very similar measuring 3 min and 9 s on the right and 2 min and 59 s on the left. The right excretion curve is slightly delayed compared with the left and the right Patlak differential function was less than the left (45% vs. 55%). Overall findings indicate that the function is relatively symmetrical with only mildly decreased function on the right relative to the left. The patient had follow-up imaging 2 years after this study, which showed that the findings were stable

Renal fusion is frequently accompanied by ectopy of the renal vessels. Because ectopic kidneys ascend and rotate less than normal kidneys, they often maintain a more primitive blood supply from the iliac vessels, lower abdominal aorta or even inferior mesenteric artery rather than assuming the mature blood supply from the mid abdominal aorta.

Horseshoe kidney

Horseshoe kidney is the most common renal fusion anomaly, accounting for 90% of all renal fusion abnormalities, with a reported incidence of approximately 1:500 live births [18]. It consists of two distinct kidneys on either side of the vertebral column that are fused most commonly at their lower poles (Fig. 2). The site of fusion is referred to as the isthmus and is usually comprised of functioning renal parenchyma or rarely a narrow band of fibrous tissue. Fusion of the two renal units of the horseshoe kidney may occur less frequently at their upper poles resulting in an inverted horseshoe kidney (5–10%), or at both poles, resulting in a disc kidney [19]. According to Cook and Stephens [20], horseshoe kidneys are further characterized as *midline* horseshoe kidneys if the fusion site between the lower poles occurs in the midline (Figs. 2 and 3), or as *laterally fused* horseshoe kidneys if the fusion site is positioned to the right or left of the vertebral

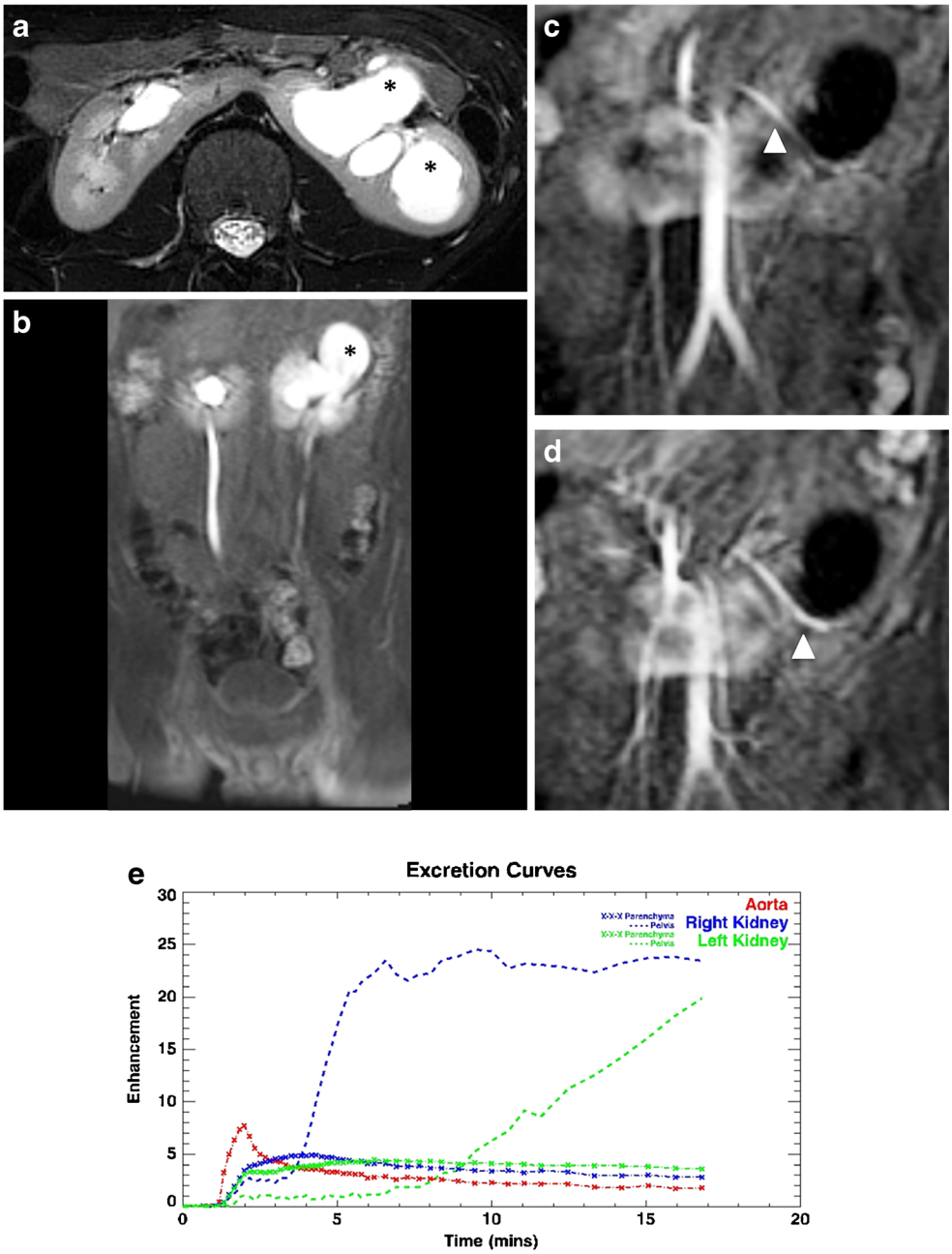

Fig. 3 A 13-year-old boy with horseshoe kidney and left renal collecting system dilation due to a crossing vessel. **a** Axial T2-weighted fat-suppressed image shows ureteropelvic junction obstruction (*asterisks*). **b** Maximum intensity projection reconstruction from a T1-weighted post-contrast fat-suppressed sequence during the excretory phase has moderate left-side pelvocaliectasis (*asterisk)* with normal caliber proximal ureter suggestive of ureteropelvic junction obstruction. **c, d** Coronal multiphase volumetric T1-weighted fat-suppressed images following gadolinium administration demonstrate a lower pole crossing renal artery *(arrowheads)* originating from the aorta causing left-side ureteropelvic junction obstruction. **e** The excretion curve on the left is markedly delayed indicating obstruction. The left renal transit time of 7 min and 13 s was delayed compared to the right, which measured 2 min and 49 s. The findings on fMRU were confirmed at surgery and the child is doing well after a dismembered pyeloplasty

column. Laterally fused systems are more commonly left dominant (70%) (Fig. 4).

Renal fusion occurs during the early stages of embryogenesis when the curved fetus undergoes progressive somatic growth and straightening. Several theories have been postulated regarding horseshoe kidney development. The widely accepted theory is that intrauterine position may impair or delay straightening of the curved fetus. This delay results in prolonged physical stress upon the embryonic renal masses within the fetal pelvis, thus delaying their ascent and predisposing them to midline fusion [5]. Another theory is that teratogens, genetic factors or chromosomal abnormalities impair normal migration of posterior nephrogenic cells that ultimately form the parenchymal isthmus [21].

The anatomical configuration of the horseshoe kidney can be complex. The horseshoe kidney is ectopic and located along the path of renal ascent, inferior to the level of the expected renal fossae because ascension is prevented by the inferior mesenteric artery [21]. In 40% of cases, the isthmus is found at the level of L3 vertebra immediately below the inferior mesenteric artery [5]. However, in the majority of cases, the isthmus lies either at the L4 level (40%) or within the pelvis (20%).

During normal development, the renal pelvises rotate from an anterior and horizontal position to a medial and vertical position. In horseshoe kidneys, fusion of the renal masses prevents this rotation. Therefore, the kidneys don't rotate and the renal pelvises remain oriented anteriorly. The ureter often inserts in a high position into the pelvis and crosses in front of the isthmus.

Horseshoe kidneys are also associated with ureteral duplication. The general population prevalence of partial ureteral duplication (bifid collecting system) is 0.6% (Fig. 4), whereas complete ureteral duplication is seen in 0.2% and may be present on one or both sides (6% are bilateral) [22, 23]. Complete ureteral duplication is most commonly associated with an ectopic ureterocele at the distal end of the upper moiety and a refluxing lower moiety [22, 23].

Horseshoe kidneys have highly variable arterial blood supply and venous drainage. Normal supply is from native renal arteries arising from the abdominal aorta. Aberrant renal arteries can arise from other mesenteric or pelvic vessels and can enter the kidney at the pelvis or directly into the poles or the isthmus of the kidney (Fig. 3) [24]. Venous anomalies associated with horseshoe kidney are also common. Multiple renal veins and variations in venous drainage have been described including retroaortic or circumaortic renal veins. Anomalous veins drain either into the inferior vena cava (IVC) or iliac veins. Variations of IVC anatomy, including double IVC, left IVC, pre-isthmic right IVC and azygos continuation of the IVC are observed ten times more frequently in association with horseshoe kidneys compared with normal kidneys (5.7%) [19, 23].

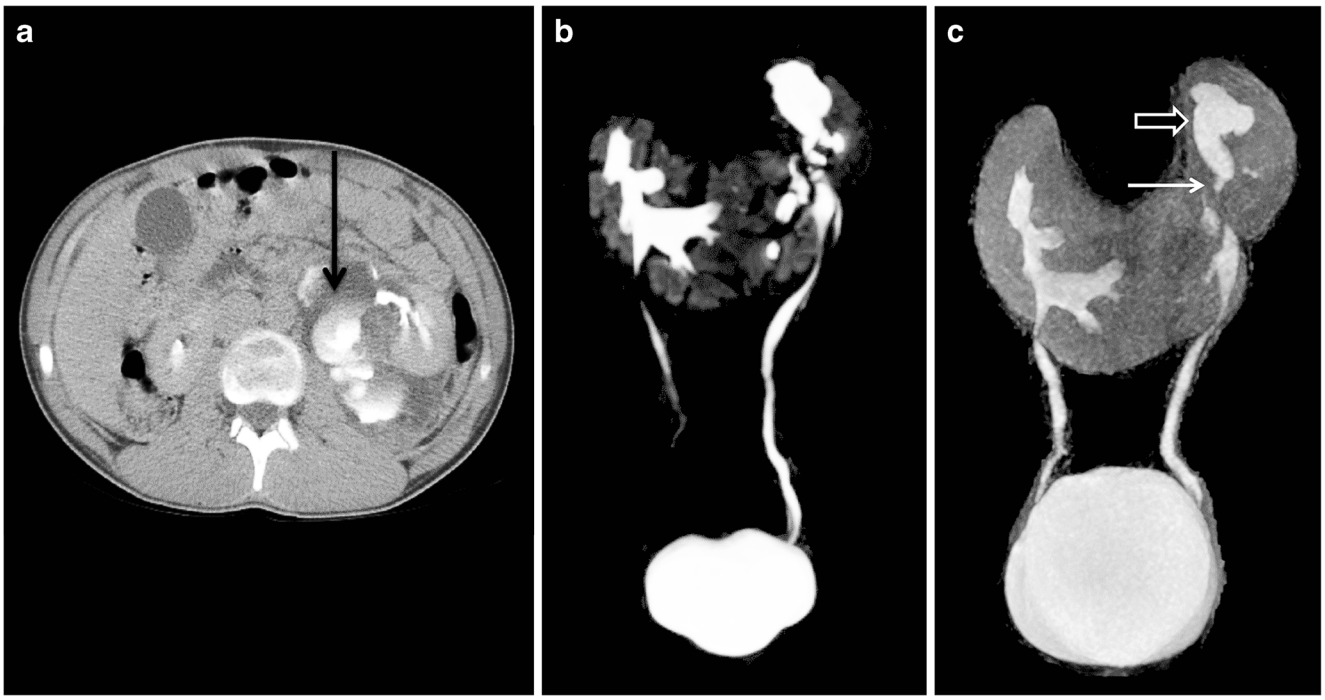

Fig. 4 Horseshoe kidney in a 17-year-old boy who had abdominal pain months after he was involved in a motor vehicle accident. **a** Delayed axial CT at the time of injury shows contrast extravasation within the left perinephric space beyond the border of the left renal collecting system *(arrow)*. **b** Several months later, the patient returned with increasing abdominal pain. Maximum intensity projection (MIP) reconstruction from an isotropic 3-D T2 fat-saturated sequence shows the left upper pole calyces are dilated and the left collecting system is dysmorphic. **c** MIP reconstruction from a T1-weighted post-contrast fat-suppressed sequence shows the horseshoe configuration of the parenchyma and scarring of the left upper pole parenchyma. It also shows an area of left upper pole infundibular post-traumatic stricture/scarring (*arrow*) and the resultant urinary tract dilation (*open arrow)*

Crossed-fused renal ectopia

Crossed-fused renal ectopia is the second most common renal fusion anomaly, with an estimated incidence of 1:1,300–1:7,500 live births [25]. In this type of ectopia, one kidney crosses over the midline and fuses with the contralateral kidney, which is located in its expected position in the renal fossa. Several subtypes of crossed-fused renal ectopia have been described based on the point of fusion between the migratory and contralateral kidney (superior, inferior or middle pole), the orientation of the crossed kidney within the abdomen and degree of the rotation of the renal pelvis. These include unilateral fused kidney with superior or inferior ectopia (Fig. 5), sigmoid or S-shaped kidney and L-shaped kidney (Fig. 6).

The most common type is the inferior renal ectopia where the lower pole of the crossing kidney fuses with the upper pole of the orthotopic kidney. The next most common type is unilateral superior ectopia where the superior pole of the crossing kidney fuses with the inferior pole of the normal kidney. In both cases, the resultant fused kidney is vertically oriented with pelvises pointed anteriorly. Left to right crossed-fused ectopy is three times more common than right to left crossover [26]. In sigmoid or S-shaped kidney, the superior pole of one kidney is fused to the inferior pole of the other kidney and the orientation remains vertical. However, the renal pelvises point in opposite directions, with the superior renal pelvis pointing medially and the inferior renal pelvis pointing laterally. In the L-shaped kidney, the superior pole of one kidney is fused to the inferior pole of the other kidney, but the orientation of the crossed kidney is horizontal within the abdomen and perpendicular to the normal vertical kidney. In all types of crossed-fused renal ectopia, the ureters most often have normal anatomical insertions into the urinary bladder (Fig. 6) [27]. Figure 5 shows a single ureter originating from a crossed-fused kidney, which seems to be a rare anatomical variant [28].

Both the normally located kidney and the crossed-fused one commonly have aberrant arterial supply originating from the upper abdominal aorta in 25% of cases and from the lower aorta or iliac arteries in the remaining cases (Fig. 5) [1, 29]. The cephalad artery is less likely to be aberrant [30]. There is also increased incidence of vesicoureteral reflux, tumors, urinary tract infections and associated genetic syndromes in patients with crossed-fused renal ectopia [27, 30].

Lump or cake kidney

Lump or cake kidney is an extreme variant of the spectrum of congenital renal fusion anomalies where the entire renal substance is fused into one mass (Figs. 7 and 8). The estimated incidence is 1:65,000 to 1:375,000, accounting for 2% of all types of crossed-fused renal cases [25]. Most commonly, the lump kidney lies in the pelvis and has two separate ureters that enter the bladder orthotopically. Rarely, lump kidney can have a single ureter.

Functional magnetic resonance urography

Functional magnetic resonance urography (fMRU) is an exam that has two parts. The first part of the exam concentrates on morphology and consists of an anatomical MRI of the abdomen and pelvis. This part usually consists of sequences to look at the renal collecting systems and the renal parenchyma. High-resolution 2-D and volumetric 3-D T2-weighted images can delineate the morphology of the pelvicalyceal system and the anatomical relationships of the urinary tract; 3-D images can be used to create a variety of reconstructions (Fig. 4). Conventional T1-weighted and T2-weighted sequences combined with new techniques, such as radial sampling of k-space for motion compensation and half-Fourier acquisitions of k-space for rapid imaging, can accurately evaluate the renal parenchymal thickness, evaluate corticomedullary differentiation and identify focal or multifocal areas of cortical thinning. The multiphase acquisition of volumetric T1-weighted gradient recalled echo images during fMRU can provide information regarding the vascular supply of the kidney that is important for surgical planning. However, digital subtraction angiography (DSA) remains the gold standard for vascular mapping. The morphological part of fMRU examination can provide exquisite morphological delineation of the complex renal anatomy.

The second part of the exam concentrates on determining the differential renal function and it consists of T1-weighted post-contrast images typically acquired during a period of 15 min. The kidneys are imaged over and over again before and after contrast administration. The post-contrast images are subtracted from the pre-contrast images to isolate the appearance and flow of the contrast through the vascular system, the kidneys and the urinary collecting system. The intensity and location of the contrast can be measured from these subtracted images. From these measurements, different renal functional parameters can be calculated. The analysis package used in this paper ([Children's Hospital of Philadelphia]-fMRU) models the flow of contrast through a three-part system: vascular, renal cortex and collecting system. This analysis package calculates how much contrast flows through each kidney to calculate differential renal function and how quickly the contrast flows through to get an idea of how efficiently the nephrons in each kidney are filtering. The Patlak values calculated by the software are a rough estimate of glomerular filtration rate and are related to the kinetic constants that govern the movement of the contrast through the blood, the kidneys and the collecting systems. This information is used to calculate accurate and comprehensive evaluation of the renal function and drainage [9, 11].

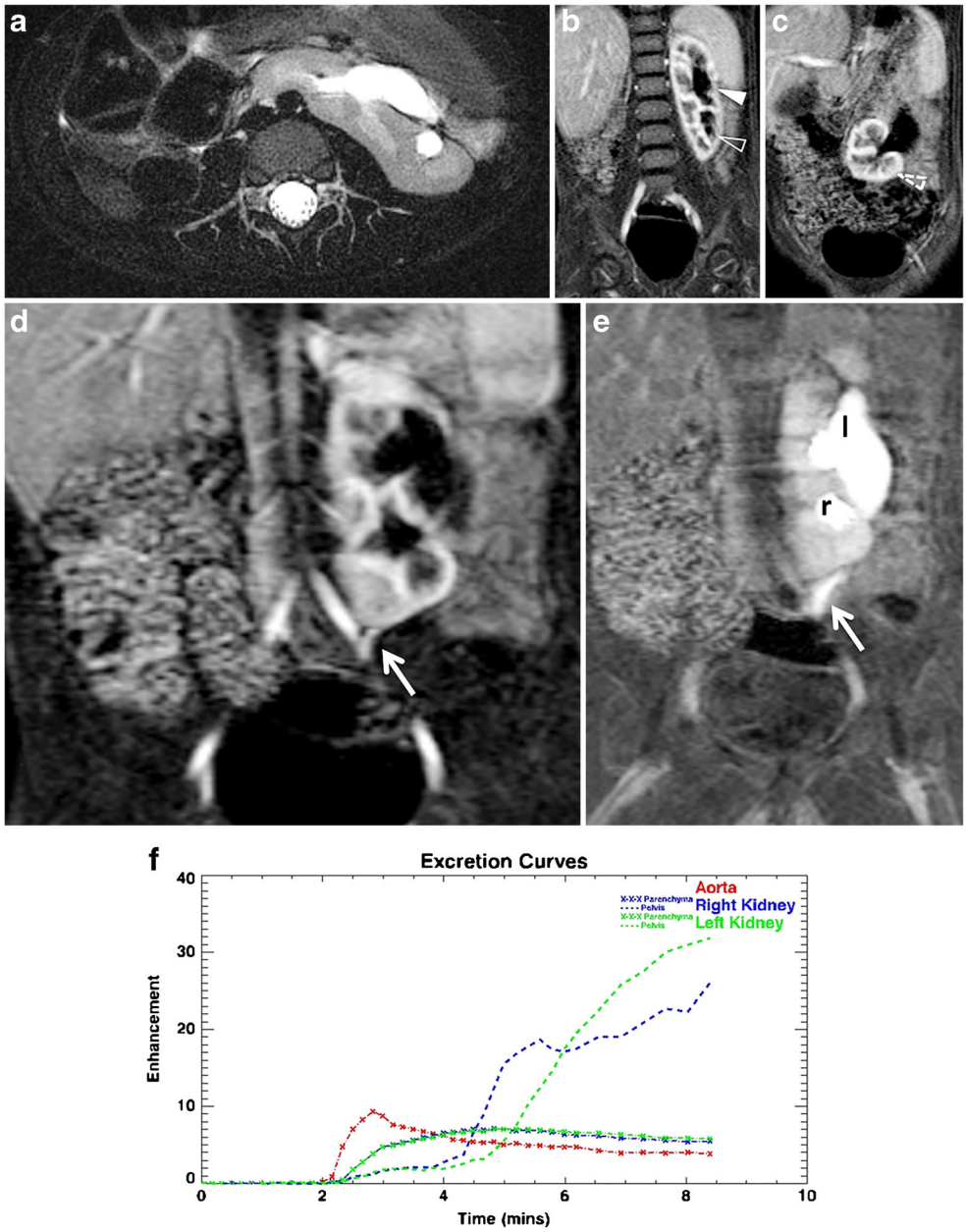

Fig. 5 A 2-year-old girl with right to left crossed-fused superior renal ectopia and grade IV vesicoureteral reflux shown by voiding cystourethrogram. **a** Axial T2-weighted fat-saturated and (**b, c**) coronal T1-weighted fat-saturated post-contrast images show the right renal moiety has crossed the midline and its superior pole (*hollow arrowhead*) has fused with the inferior pole of the left renal moiety (*solid arrowhead*), which remains in its expected anatomical location in the left renal fossa. The lower pole of the right renal moiety extends to the midline (*dashed arrowhead*). The right renal moiety does not have a separate ureter, but communicates with the collecting system of the left renal moiety as a bifid system. **d** Coronal T1-weighted fat-saturated post-contrast image during the arterial phase shows an aberrant renal artery (*arrow*) supplying the mid-lower pole of the left renal moiety, originating from the left common iliac artery. **e** Coronal T1-weighted fat-saturated post-contrast image during the excretory phase shows mild caliectasis of both moieties (l=left and r=right). There is no ureterectasis. The distal left ureter (*arrow*) is oriented toward the left side of the bladder. **f** Note the steady increase in the bilateral excretion curves from the functional analysis indicative for vesicoureteral reflux. The enhancement curves are symmetrical and the cortical transit times are almost equal (right is 2:19 and left is 2:29) with 51% Patlak differential renal function on the right and 49% Patlak differential renal function on the left. All of the preceding findings indicate no obstruction

Complications of renal fusion anomalies

Horseshoe and crossed-fused kidneys are usually asymptomatic and most commonly detected incidentally during routine prenatal or postnatal imaging examinations [31]. However, patients with these anomalies are predisposed to numerous pathological conditions and complications, including renal parenchyma dysplasia, ureteropelvic junction obstruction,

Fig. 6 An 11-month-old girl with left to right L-shaped crossed-fused renal ectopia and urogenital sinus. **a** Three-dimensional reformat of maximum intensity projection coronal T2-weighted fat-suppressed image shows the right renal moiety is located in the expected anatomical location in the right renal fossa. The left renal moiety has a horizontal orientation and crossed the midline with its superior pole fused to the inferior pole of the right renal moiety. The left (*hollow arrowhead*) and right (*arrowhead*) ureters insert orthotopically into the bladder. **b** Axial T2-weighted fat-saturated image shows the renal parenchyma of both kidneys (*arrowhead*=right, *arrow*=left) is normointense with normal corticomedullary differentiation and no cortical thinning. **c** Sagittal T2-weighted fat-saturated image shows the position of the vagina, marked by the catheter (*arrow*). **d** Sagittal T1-weighted fat-saturated post-contrast image shows a normal-appearing bladder neck with a dilated proximal urethra (*dashed arrow*). At the end of this structure, there was a small stenotic-appearing opening that corresponded to the confluence of urethra and the vagina (*arrow*) into the urogenital sinus (*arrowhead*). These findings were confirmed by cystoscopy

ectopic ureteral insertion, ureterovesical junction obstruction, vesicoureteral reflux, renal infections, urolithiasis, traumatic injury and neoplasia [18, 27, 31].

Ureteropelvic junction obstruction

In renal fusion and ectopia, there is a higher incidence of ureteropelvic junction (UPJ) obstruction. Early and accurate recognition of this condition and surgical correction of significant obstruction is important to prevent irreversible renal damage. Specific causes include congenital narrowing, abnormal position and orientation of the renal pelvis, abnormal ureteral course or vessels crossing over the renal pelvis. UPJ obstruction is a common congenital abnormality leading to urological surgery in children (Fig. 3).

In horseshoe kidneys with UPJ obstruction, the anatomical part of the fMRU is useful in demonstrating the

Fig. 7 A 2-month-old girl with pelvic lump kidney and congenital hydronephrosis. **a** Coronal high-resolution T2-weighted fat-saturated image shows fused pelvic kidney with a horizontal orientation. The left renal moiety is significantly larger than the right. Both renal moieties have vertically oriented renal pelvises (*asterisks*) that are directed inferiorly. There is severe left ureterectasis with a tortuous redundant morphology left ureter (*arrowheads*) that inserts within the left paramedian bladder base and is associated with a large ureterocele (*arrow*). **b** Axial high-resolution T2-weighted fat-saturated image. Scattered small simple renal cortical cysts (*arrowhead*) are noted near the each pelvis. **c** Sagittal high-resolution T2-weighted fat-saturated image shows that posterior to the bladder (*arrow*) there is a fluid-filled structure (*star*) that corresponds to a dilated vagina. This joins with the distal urethra into a common channel (not shown) in keeping with urogenital sinus. **d,e** Sagittal T1-weighted fat-saturated post-contrast images during the excretory phase were useful in localizing the right ureter (*hollow arrowheads*), which inserted ectopically into the proximal urogenital sinus. These findings were confirmed during cystoscopy

morphology and orientation of the renal pelvis and the relationship to the flow voids of surrounding vessels [24]. The ureteropelvic junction is located higher than normal and the ureter usually courses anteriorly to the isthmus. In the case of crossed-fused renal ectopia, fluid-sensitive sequences can define the borders of the fused renal moieties and determine the type of fusion.

The functional part of fMRU and post-processing analysis help demonstrate delayed or absent drainage of the contrast and the variable degree of associated renal functional impairment in the case of decompensated UPJ obstruction. Post-processing analysis can quantify the differential renal function parameters using the kinetics of contrast uptake and excretion. In addition, the functional part of fMRU can help differentiate between non-obstructive pelvocaliectasis and clinically relevant UPJ obstruction. For example, the patients in Figs. 2 and 3 have unilaterally dilated renal pelvises. In Fig. 3, the patient had symmetrical excretion on post-contrast images and very similar cortical transit times and Patlak values. In Fig. 4, the dilated left pelvis had delayed excretion of

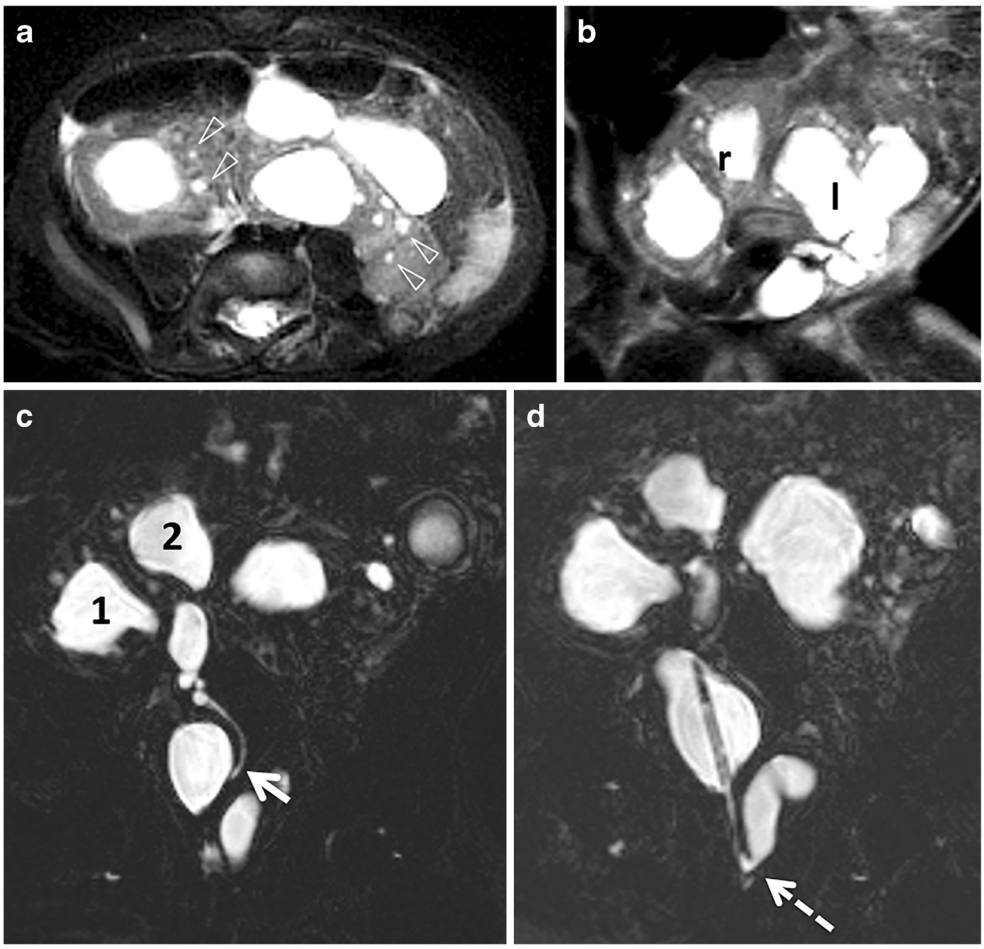

Fig. 8 A 12-day-old girl with VACTERL and cystic lump kidney. Axial (**a**) and coronal (**b**) T2-weighted fat-suppressed high-resolution images show an enlarged midline kidney with the right (r) and left (l) renal moieties joined centrally in the lower pelvis. The renal parenchyma contains numerous tiny cortical cysts (*open arrowheads*). Coronal T2-weighted fat-suppressed high-resolution image (**c**) shows that the right renal moiety has a bifid configuration (1 + 2) with severe pelvocalliectasis. The right ureter crosses the midline and inserts in an ectopic position in the left bladder wall (*arrow*). Coronal T2-weighted, fat-suppressed high-resolution image (**d**) shows left renal moiety with diffuse pelvocalliectasis. The left ureter has an ectopic extravesical insertion in the distal urethra (*dashed arrow*)

contrast and the left cortical transit time was delayed compared with the right.

Occasionally, a lower pole renal vessel crossing over the renal pelvis may cause extrinsic obstruction of the ureteropelvic junction. In this case, the arterial phase of the dynamic post-contrast volumetric T1-weighted sequence can reveal the crossing vessel and establish the diagnosis (Fig. 3).

Vesicoureteral reflux

Vesicoureteral reflux (VUR) is frequently associated with renal fusion anomalies. Cascio et al. [32] found that 13/40 (32%) horseshoe kidney patients had VUR on voiding cystourethrograms. Similarly, in a study by Solanki et al. [26] that included six children with crossed-fused renal anomalies, vesicoureteral reflux was detected in four cases and ureteric reimplantation was required in three children [26].

The imaging modalities of choice to detect VUR and evaluate its severity are voiding cystourethrography, nuclear medicine cystogram and contrast-enhanced voiding urosonography. However, fMRU can exquisitely demonstrate retrograde urine flow and the sequelae of recurrent urinary tract infections such as pyelonephritis and renal scarring. The advantage for fMRU over planar nuclear medicine images in assessing the thickness of the renal cortex is particularly important given that the complex anatomy of the renal fusion anomalies can impede the evaluation of the renal parenchyma with US. Renal scarring appears as focal or multifocal areas of cortical thinning overlying a renal pyramid. fMRU has been shown to have higher interobserver agreement and higher accuracy than dimercaptosuccinic acid (DMSA) for identifying renal parenchyma defects [32]. Upward spikes or increasing signal intensity in the collecting systems are also a good indication of VUR on the functional part of the fMRU exam (Fig. 6) [32].

Urinary tract calculi

Urinary tract calculi can be frequently associated with renal fusion anomalies. They result from prolonged urinary stasis or infections and are associated with pelvicalyceal dilation or obstruction [24, 33].

Stones within the urinary tract can be identified on conventional MRI sequences of fMRU examination as signal voids on T2-weighted images, surrounded by urine that is of high signal (Fig. 9). Post-contrast T1-weighted images are useful in

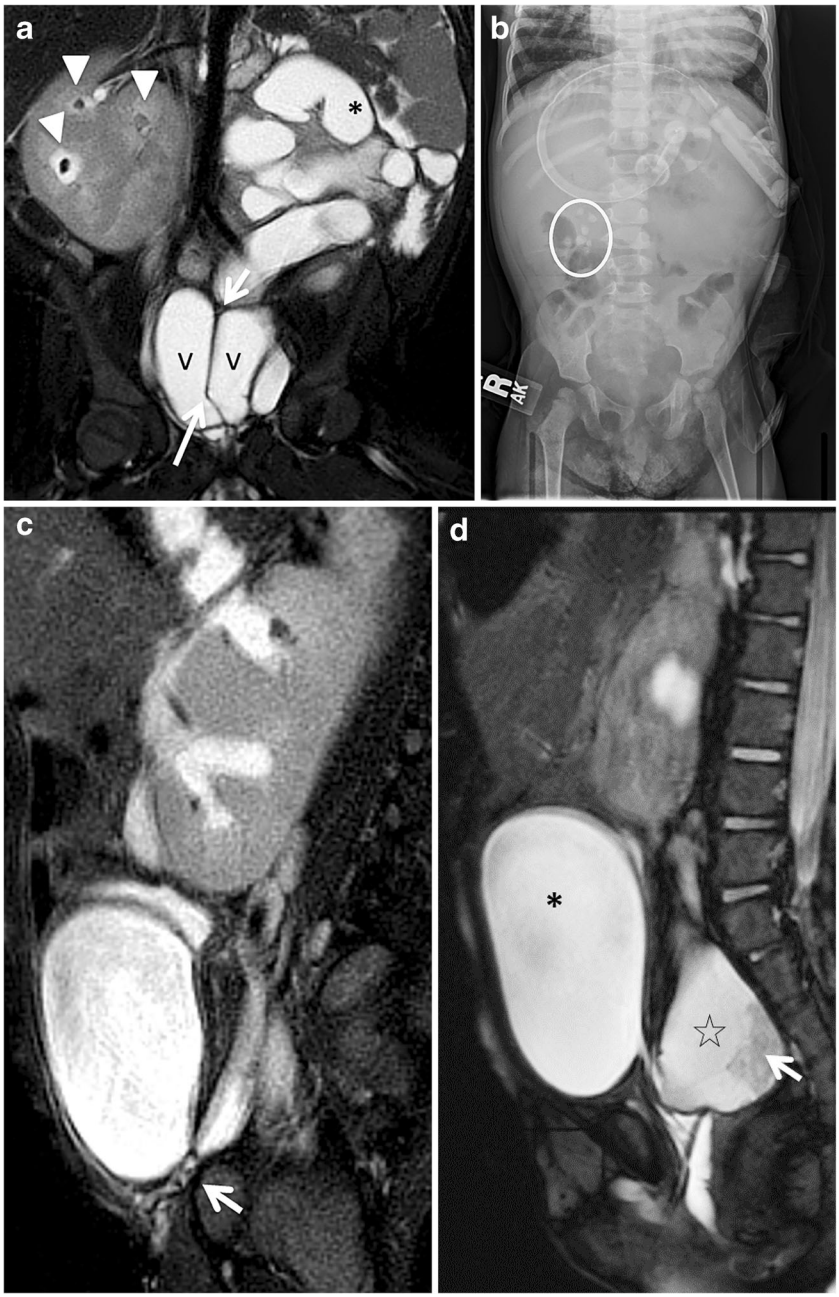

Fig. 9 Horseshoe kidney in a 1-year-old girl with VACTERL, renal stones and left renal dysfunction. Coronal T2-weighted fat-saturated image (**a**) showing multiple low signal intensity foci is seen within calyces on the right side and surrounded by fluid signal (urine) representing renal calculi (*arrowheads*). There is marked left urinary tract dilation *(asterisk)* with severe parenchymal thinning. Markedly dilated vagina with hemivaginas (*v*) and longitudinal septum *(arrows)*. Corresponding abdominal radiograph (**b**) also demonstrates the right renal stones (circle). Sagittal T2-weighted fat-saturated image (**c**) shows ectopic insertion of right ureter in the inferior aspect of the bladder (*arrow*). Sagittal T2-weighted fat-saturated image (**d**) of a septated fluid-filled structure that represents one horn of the vagina *(star)* posterior to the urinary bladder *(asterisk)*. The degree of fluid retention within the vagina suggests vaginal outlet obstruction. A fluid-debris level *(arrow)* seen within the right hemi-vagina was secondary to communication with the gastrointestinal tract. Intraoperatively, a complete fusion of the rectum, urethra and vagina was found indicating the cloacal malformation

identifying stones using high contrast differentiation between excreted contrast in the urinary tract and the low signal of renal calculi. Post-contrast images and functional data can assess for the possibility of concurrent UPJ obstruction. If there is concurrent UPJ obstruction, a pyeloplasty would be performed at the same time as a pyelolithotomy.

Ureteral duplication, ectopic ureteral insertion and other abnormalities of the urogenital tract

Complete or partial ureteral duplication (Fig. 4) and ectopic ureteral insertion into adjacent pelvic structures such as the urethra, vagina or seminal vesicles (Figs. 7 and 8)

are commonly associated with renal fusion and ectopia [34, 35].

Renal fusion and ectopia can also be associated with other congenital abnormalities of the urogenital tract such as urogenital sinus and cloacal malformations (Fig. 9) or as part of VACTERL (vertebral defects, anal atresia, cardiac defects, tracheoesophageal fistula, renal anomalies, and limb abnormalities) (Figs. 8 and 9) or Turner syndrome [27].

High-resolution T2-weighted anatomical images coupled with post-contrast excretory volumetric images can delineate the pelvicalyceal system morphology and detect the exact number and insertion point of a contrast-filled ureter and define pelvic anatomy (Fig. 7). This anatomical detail is crucially important if surgical repair is planned.

Blunt abdominal trauma

Traumatic renal injury of a patient with renal fusion anomaly may occur in the setting of blunt abdominal trauma and can be serious even with minor impact forces. The horseshoe kidney is lower and relatively anterior in the abdomen and, therefore, not protected by the lower rib cage making it susceptible to parenchymal lacerations and ureteric injuries (Fig. 4). In addition, the isthmus is more vulnerable to compression injuries against the lumbar vertebrae as it is closely opposed to the spine. Rupture or transection of the isthmus has been reported [7, 36]. Contrast-enhanced multidetector CT is typically the modality of choice for evaluating trauma patients; however, fMRU can be used in the follow-up of these cases or in cases managed conservatively.

Malignancy

Wilms tumor occurs with increased incidence in patients with horseshoe kidneys. Neville et al. [38] showed that the prevalence of Wilms tumor is 1.76 to 7.93 times higher in those with horseshoe kidneys compared to the general population (Fig. 10). The isthmus is the most common location for tumor development. This may be explained based on the theory that the isthmus is formed as the result of teratogenic effect on the metanephric blastema during embryogenesis leading to abnormal proliferation [24].

Wilms tumor arising in a horseshoe kidney presents a unique diagnostic and surgical challenge because the large tumor can often overshadow the underlying fusion abnormality. The underlying fusion anomaly was missed on preoperative imaging in seven patients in a series of 22 patients with

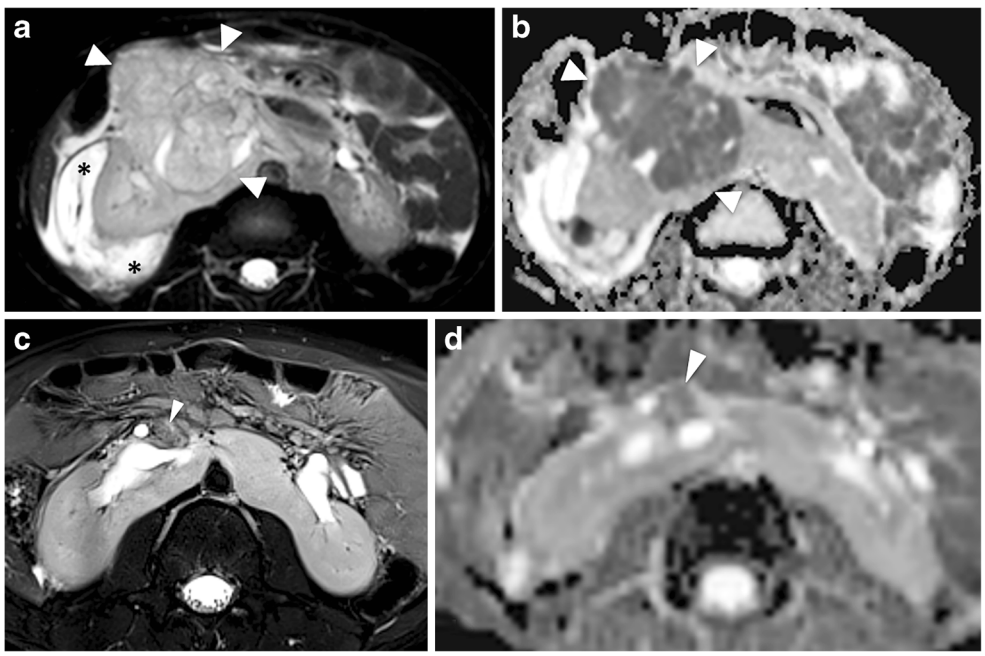

Fig. 10 An 8-year-old boy with horseshoe kidney with a Wilms tumor. High-resolution T2-weighted image (**a**) with fat saturation shows a lobular heterogeneously hyperintense mass (*arrowheads*) centered within the lower pole of the right renal moiety extending across the midline toward the isthmus. There is associated complex right perinephric fluid collection (*asterisks*) suggestive of perinephric urinoma. The mass (*arrowheads*) demonstrates restricted diffusion on the (**b**) apparent diffusion coefficient (ADC) map. The patient then underwent adjuvant chemotherapy before surgical resection to shrink the tumor. Axial T2-weighted fat-suppressed high-resolution image (**c**) after chemotherapy shows decreased size of the mass (*arrowhead*). The residual tumor (*arrowhead*) demonstrates restricted diffusion on the ADC map (**d**). The tumor was subsequently completely removed with resection of the isthmus of tissue joining the two renal moieties

Wilms tumor. Four of these seven patients had ultrasounds and/or CT and three of these patients only had abdominal radiography or excretory urography. Note that the CTs were all performed prior to 1997 and modern CT would likely have been able to diagnose the underlying fusion abnormality. fMRU could be a helpful adjunct in cases where patients only have preoperative ultrasounds and/or radiographic images [37].

fMRU is helpful in the surgical planning of nephrectomy by delineating the exact borders of the two renal moieties and their anatomical relationships with the mass. It can also help in accurate staging by revealing lymphadenopathy. fMRU has also been used for assessing tumor response if a patient initially receives adjuvant therapy and for surveilling residual or recurrent tumor after the primary tumor has been resected.

Conclusion

Renal fusion anomalies are a complex group of congenital anomalies of the kidney and urinary tract. Although they can be asymptomatic and detected incidentally, they are often associated with complications, such as obstruction, vesicoureteric reflux, renal calculi, trauma or, rarely, malignancy. fMRU is a highly sensitive and radiation-free imaging modality that can provide detailed morphological and functional information that can facilitate the care and management of children with renal fusion anomalies.

Compliance with ethical standards

Conflicts of interest None

References

1. Turkvatan A, Olcer T, Cumhur T et al (2009) Multidetector CT urography of renal fusion anomalies. Diagn Interv Radiol 15:127–134
2. Volkan B, Ceylan E, Kiratli PO et al (2003) Radionuclide imaging of rare congenital renal fusion anomalies. Clin Nucl Med 28:204–207
3. Muttarak M, Sriburi T (2012) Congenital renal anomalies detected in adulthood. Biomed Imaging Interv J 8:e7
4. Patel TV, Singh AK (2008) Crossed fused ectopia of the kidneys. Kidney Int 73:662
5. Friedland GW, de Vries P (1975) Renal ectopia and fusion. Embryologic Basis Urology 5:698–706
6. Yohannes P, Smith AD (2002) The endourological management of complications associated with horseshoe kidney. J Urol 168:5–8
7. Heredero Zorzo O, Palacios Hernandez A, Eguiluz Lumbreras P et al (2009) Horseshoe kidney rupture. Arch Esp Urol 62:131–133
8. McAleer IM, Kaplan GW, LoSasso BE et al (2002) Congenital urinary tract anomalies in pediatric renal trauma patients. J Urol 168:1808–1810
9. Darge K, Higgins M, Hwang TJ et al (2013) Magnetic resonance and computed tomography in pediatric urology: an imaging overview for current and future daily practice. Radiol Clin N Am 51:583–598
10. Darge K, Anupindi SA, Jaramillo D et al (2011) MR imaging of the abdomen and pelvis in infants, children, and adolescents. Radiology 261:12–29
11. Khrichenko D, Darge K (2010) Functional analysis in MR urography - made simple. Pediatr Radiol 40:182–199
12. Dias T, Sairam S, Kumarasiri S et al (2014) Ultrasound diagnosis of fetal renal abnormalities. Best Pract Res Clin Obstet Gynaecol 28: 403–415
13. Rowell AC, Sangster GP, Caraway JD et al (2012) Genitourinary imaging: part 1, congenital urinary anomalies and their management. AJR Am J Roentgenol 199:W545–W553
14. Little M, Georgas K, Pennisi D et al (2010) Kidney development: two tales of tubulogenesis. Curr Top Dev Biol 90: 193–229
15. Michos O (2009) Kidney development: from ureteric bud formation to branching morphogenesis. Curr Opin Genet Dev 19:484–490
16. Angtuaco TL, Collins HB, Quirk JG et al (1999) The fetal genitourinary tract. Semin Roentgenol 34:13–28
17. Cohen HL, Kravets F, Zucconi W et al (2004) Congenital abnormalities of the genitourinary system. Semin Roentgenol 39:282–303
18. Weizer AZ, Silverstein AD, Auge BK et al (2003) Determining the incidence of horseshoe kidney from radiographic data at a single institution. J Urol 170:1722–1726
19. Bozdogan E, Demir M, Konukoglu O et al (2016) Reverse U-shaped horseshoe kidney accompanied by gibbus deformity and spina bifida. Jpn J Radiol 34:448–450
20. Cook WA, Stephens FD (1977) Fused kidneys: morphologic study and theory of embryogenesis. Birth Defects Orig Artic Ser 13:327–340
21. Natsis K, Piagkou M, Skotsimara A et al (2014) Horseshoe kidney: a review of anatomy and pathology. Surg Radiol Anat 36:517–526
22. Singh SK, Kumar A (2015) Bilateral partial duplex collecting system in horseshoe kidney with stone in the left upper and lower moiety: an unusual association. Saudi J Kidney Dis Transpl 26: 608–610
23. Taghavi K, Kirkpatrick J, Mirjalili SA et al (2016) The horseshoe kidney: surgical anatomy and embryology. J Pediatr Urol 12:275–280
24. O'Brien J, Buckley O, Doody O et al (2008) Imaging of horseshoe kidneys and their complications. J Med Imaging Radiat Oncol 52: 216–226
25. Miclaus GD, Pupca G, Gabriel A et al (2015) Right lump kidney with varied vasculature and urinary system revealed by multidetector computed tomographic (MDCT) angiography. Surg Radiol Anat 37:859–865
26. Solanki S, Bhatnagar V, Gupta AK et al (2013) Crossed fused renal ectopia: challenges in diagnosis and management. J Indian Assoc Pediatr Surg 18:7–10
27. Guarino N, Tadini B, Camardi P et al (2004) The incidence of associated urological abnormalities in children with renal ectopia. J Urol 172:1757–1759
28. Kaur N, Saha S, Mriglani R et al (2013) Crossed fused renal ectopia with a single ureter: a rare anomaly. Saudi J Kidney DisTranspl 24: 773–776
29. Bailey SH, Mone MC, Nelson EW et al (2002) Transplantation of crossed fused ectopic kidneys into a single recipient. J Am Coll Surg 194:147–150
30. Glodny B, Petersen J, Hofmann KJ et al (2009) Kidney fusion anomalies revisited: clinical and radiological analysis of 209 cases of crossed fused ectopia and horseshoe kidney. BJU Int 103:224–235

31. Je BK, Kim HK, Horn PS et al (2015) Incidence and spectrum of renal complications and extrarenal diseases and syndromes in 380 children and young adults with horseshoe kidney. AJR Am J Roentgenol 205:1306–1314
32. Cerwinka WH, Grattan-Smith JD, Jones RA et al (2014) Comparison of magnetic resonance urography to dimercaptosuccinic acid scan for the identification of renal parenchyma defects in children with vesicoureteral reflux. J Pediatr Urol 10:344–351
33. Ghosh BC, DeSantis M, Kleyner Y et al (2008) Crossed fused renal ectopia with calculi. J Am Coll Surg 206:753
34. Kraft KH, Molitierno JA, Kirsch AJ et al (2007) Ten-year-old girl with crossed-fused ectopic kidney and ectopic ureter to vagina. Urology 70:1220–1221
35. Lin VC, Weng HC, Kian-Lim E et al (2010) An atrophic crossed fused kidney with an ectopic vaginal ureter causing urine incontinence. Urology 76:55–56
36. Dominguez K, Ekeh AP (2011) Blunt trauma causing transection of a horseshoe kidney. J Trauma 71:517
37. Huang EY, Mascarenhas L, Mahour GH et al (2004) Wilms tumor and horseshoe kidneys: a case report and review of the literature. J Pediatr Surg 39:207–212